Available online at www.sciencedirect.com
ScienceDirect
Ceramics International 40 (2014) 4323–4326
CERAMICS INTERNATIONAL
www.elsevier.com/locate/ceramint

High energy-storage properties of $[(Bi_{1/2}Na_{1/2})_{0.94}\ Ba_{0.06}]\ La_{(1-x)}\ Zr_xTiO_3$ lead-free anti-ferroelectric ceramics

Yongfeng Wang[a,b,*], Zhenlin Lv[a], Hui Xie[b], Jing Cao[b]

[a]School of Materials Science and Engineering, Xi'an University of Technology, Xi'an 710048, PR China
[b]School of Mechanical Engineering, Xi'an Aeronautical University, Xi'an 710077, PR China

Received 13 August 2013; received in revised form 20 August 2013; accepted 22 August 2013
Available online 8 September 2013

Abstract

Energy-storage properties of $[(Bi_{1/2}Na_{1/2})_{0.94}Ba_{0.06}]La_{(1-x)}Zr_xTiO_3$ (BNT-BLZT, $x=0$, 0.02, 0.04, and 0.06) lead-free anti-ferroelectric ceramics fabricated via the conventional sintering technique were first investigated. Calculation from the X-ray diffraction results reveals that BNT-BLZT ceramic possesses a single perovskite structure phase. In addition, the *P–E* hysteresis loops measured at room temperature show that the BNT-BLZT ($x=0.02$) ceramics obtain the maximum P value of 37.5 μC/cm^2 and the largest energy-storage density W_{max} is 1.58 J/cm^3. The temperature dependence of dielectric permittivity ε_r and dielectric loss tanδ illustrate that the addition of Zr can improve the piezoelectric properties of BT-BLZT ceramics. These properties indicate that BNT-BLZT ceramics might be a promising lead-free anti-ferroelectric material for energy storage application.

Keywords: A. Ceramics; C. X-ray diffraction; D. Energy storage

1. Introduction

Piezoelectric ceramics are widely used in various applications such sensors and capacitors. Capacitors are a key component in pulse power circuits utilized to produce large amounts of electrical energy within an extremely short time span. With the increasing demands for compact electronics, high energy-storage density dielectric materials become a major enabling technology [1–3]. Studies have shown that anti-ferroelectric (AFE) materials have higher energy-storage density and better dielectric properties than ferroelectric (FE) materials [4,5]. However, AFE materials that have been extensively studied are mostly lead-based, such as PZST, PLZT, and PLZ, with the highlights of the global environmental problems, environment-friendly materials will become the mainstream demand for future development [6].

As a lead-free piezoelectric material, BNT-BT has drawn increasing attention in these years [7]. It was reported to exhibit a morphotropic phase boundary at approximately 6 mol% BT separating the rhombohedral BNT-rich side and the tetragonal BT-rich side [8]. Between 0% and 15 mol% BT, there is a transition from a FE phase into an AFE phase at higher temperatures, with the transition lying at about 140 °C at the morphotropic phase boundary [9]. Recently, Zhang et al. lowered the transition temperature by introducing KNN into BNT-BT system and obtained BNT-BT-KNN materials with "slanted" *P–E* hysteresis loops [10–12]. The AFE materials with "square" hysteresis loops generally possess higher energy-storage density than those with "slanted" ones [13–15]. But, it is very difficult for the AFE materials with "square" hysteresis loops to withstand over several hundred charge–discharge circulations, because it is often cracked due to the phase transition in the charge–discharge circulations, more "slanted" hysteresis loops and smaller area of hysteresis loops will be helpful to the charge–discharge circulations [16–18]. However, so far, there is lack of reports on the energy-storage properties of AFE materials. Gao et al. reported energy-storage properties of the AFE material, but the largest energy-storage density W_{max} is 0.59 J/cm^3 [19,20]. In this paper, the energy-storage properties of BNT-BLZT ceramics were firstly studied to unveil its potential for energy-storage application.

*Corresponding author at: School of Materials Science and Engineering, Xi'an University of Technology, Xi'an 710048, PR China. Tel./fax: +86 29 84252696.
E-mail address: wangyfeng@163.com (Y. Wang).

0272-8842/$ - see front matter © 2013 Elsevier Ltd and Techna Group S.r.l. All rights reserved.
http://dx.doi.org/10.1016/j.ceramint.2013.08.099

2. Experimental

By a conventional ceramic sintering technique, the $[(Bi_{1/2}Na_{1/2})_{0.94}Ba_{0.06}]La_{(1-x)}Zr_xTiO_3$ (BNT-BLZT) ceramics were prepared using Bi_2O_3(99%, 465.96), Na_2CO_3(99.8%, 105.99), $BaCO_3$(99%, 197.34), TiO_2(98%, 79.87), ZrO_2(99%, 123.22) and La_2O_3 (99.99%, 325.81) as starting raw materials. Firstly, the starting materials were weighed according to the stoichiometric formula and then mixed in ethanol with zirconium balls by ball-milling for 6 h, dried, sieved, pressed into cylinder. Secondly, the cylinders were calcined at 1000 °C for 6 h in air. The cylinders calcined were again ball-milled, sieved, and pressed into disks with diameter of 10 mm and thickness of 1 mm by dry pressuring. To minimize the evaporation of the volatile elements Bi, and Na, the disks were buried in a powder of the same composition. Finally, the compacted disks were sintered in air at 1150 °C for 4 h. Silver slurry was coated on both sides of the disks, then dried at 850 °C for 30 min, polished its cylindrical surface as electrodes.

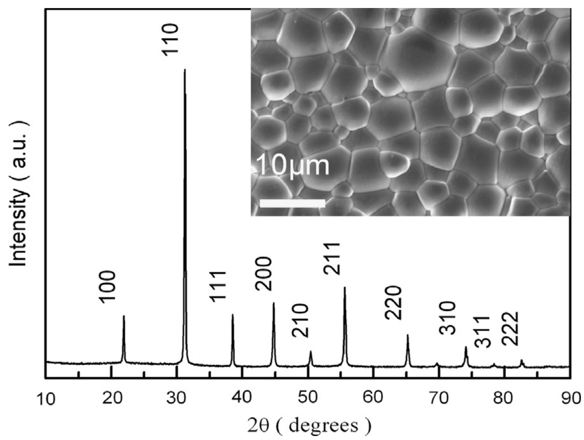

Fig. 1. The XRD patterns of the $[(Bi_{1/2}Na_{1/2})_{0.94}Ba_{0.06}]La_{(1-x)}Zr_xTiO_3$ ceramics. The inset shows the microstructure of the polished $[(Bi_{1/2}Na_{1/2})_{0.94}Ba_{0.06}]La_{(1-x)}Zr_xTiO_3$ ceramics surface.

2.1. Characterization

X-ray diffraction (XRD) patterns of the ceramics were performed using Cu Kα radiation in the θ-2θ scan mode (X'Pert PRO). The microstructures were observed using scanning

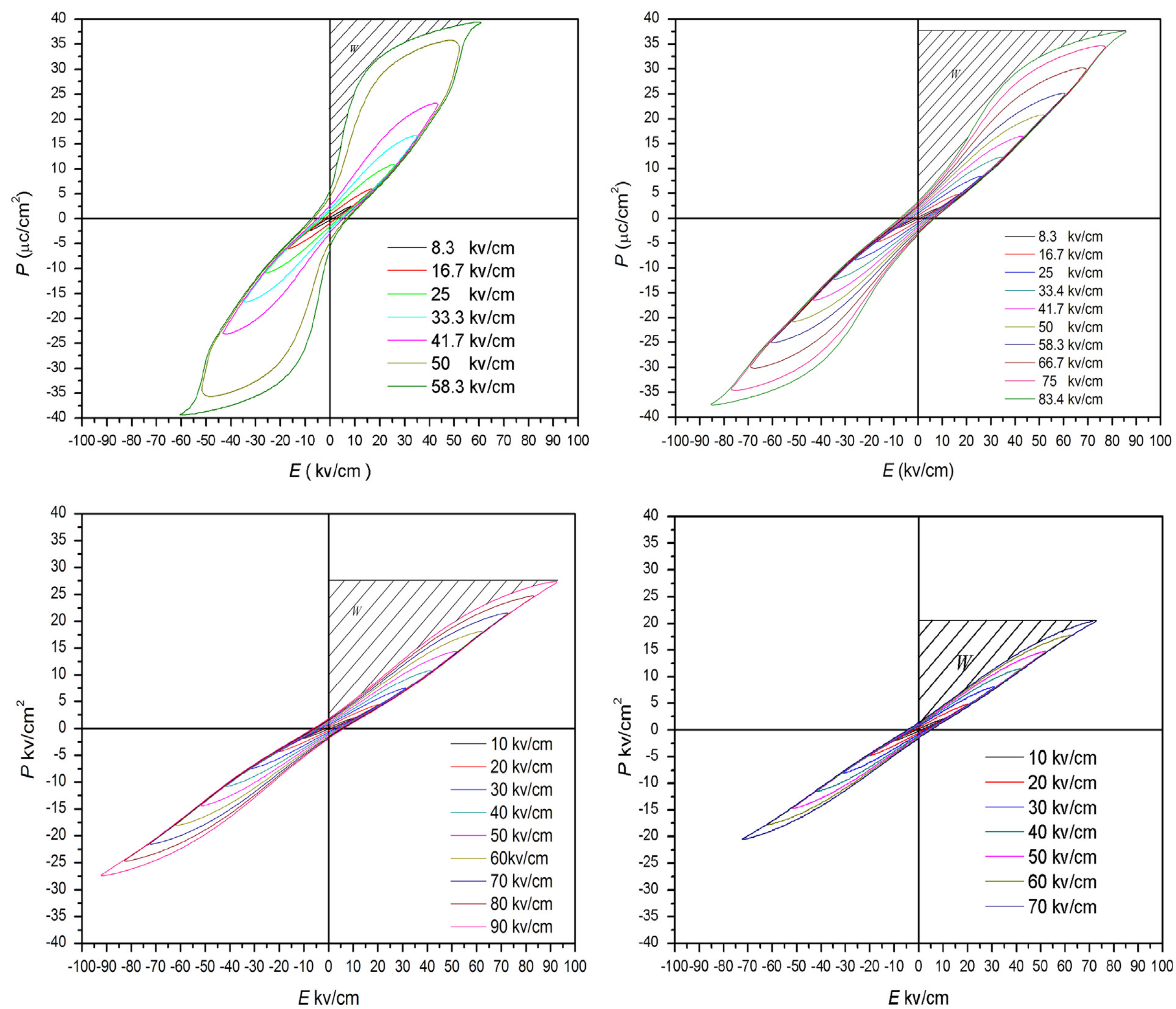

Fig. 2. The P–E hysteresis loops of BNT-BLZT ceramics under different electric fields at room temperature.

electron microscopy (SEM, S440). The saturation polarization (P_s), the remanent polarization (P_r) and coercive field (E_c) were determined from polarization versus electric field (P–E) hysteresis loops measured by a Radiant Precision Workstation (USA). The dielectric permittivity (ε_r) and dielectric loss (tan δ) of the samples were measured using an impedance analyzer at 100 Hz, 1 kHz, 10 kHz, 100 kHz and 1 MHz (HP 4278A).

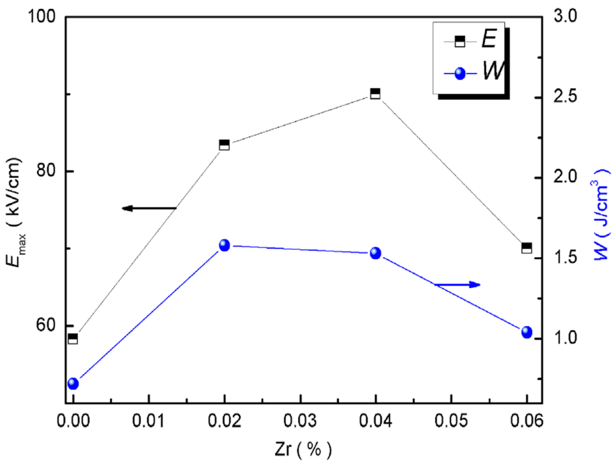

Fig. 3. The W–E curves of maximum electric field intensity E_{max} and energy-storage density W.

3. Results and discussion

Fig. 1 shows the XRD result of the BNT-BLZT(x=0.02) ceramics and the inset illustrates the microstructure of the polished and acid-etched surface. All the peaks could be indexed based on a tetragonal perovskite structure. It can be seen that the ceramic possesses a single perovskite structure phase, indicating that Zr^{4+} can diffuse into the BNT-BLT lattices to form a solid solution. The SEM image of BNT-BLZT ceramics inserted in Fig.1 shows that the average grain size is about 10 μm, the grain boundaries are clear, and no obvious visible pores can be found. The patterns indicate that the ceramics are crystallized into a single perovskite structure phase.

Fig. 2 shows the P–E hysteresis loops of BNT-BLZT ceramics under different electric fields at 1 Hz. It can be observed that the saturated polarization P_s and the remnant polarization P_r both decreased with an increase of Zr content. The P–E hysteresis loops are observed that P_s is 40 μC/cm^2 at x=0. P_s is 20.8 μC/cm^2 with x=0.06, and the P–E hysteresis loops of BNT-BLZT ceramics increasingly becomes more slant and slim. It can be observed that P_s and P_r both decreases as the increase of Zr doped.

To further investigate the electric field strength dependence on the energy-storage density, the W–E curves measured at the room temperature is given in Fig. 3, which shows the maximum electric field intensity E_{max} and energy-storage density W of the ceramics as a function of x. The shaded areas in Fig. 2 display

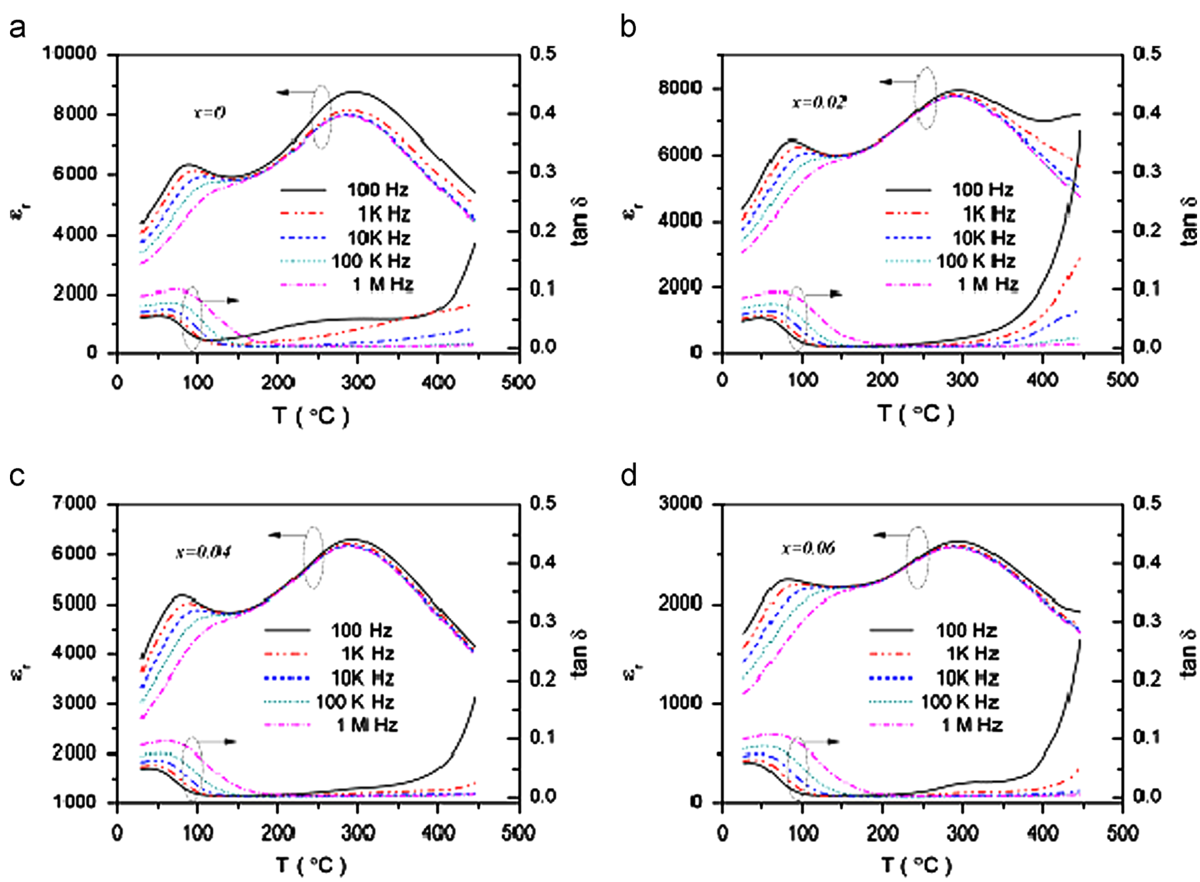

Fig. 4. Temperature-dependent dielectric permittivity (ε_r) and dielectric loss (tanδ) of BNT-BLZT ceramics measured at different frequencies.

energy-storage density of BNT-BLZT ceramics, the larger shaded areas is, the better energy-storage properties are. The energy-storage density W can be calculated according to Eq. (1), E is electric field intensity. The maximum electric field intensity E_{max} and the energy-storage density W is first increased and then decreased with the Zr doped increasing from 0 to 0.06. But when $x=0.02$, the largest energy-storage density W_{max} is 1.58 J/cm^3, and $E_c=83.4$ kV/cm.

$$W = \int_{P_r}^{P_s} E\, dp, 0 \le E \le E_{\max} \quad (1)$$

Fig. 4 (a)–(d) shows that the temperature dependence of dielectric permittivity ε_r and dielectric loss tanδ of poled BNT-BLZT ceramics with $x=0$, 0.02, 0.04 and 0.06, respectively, at different frequencies ranging from 100 to 1 MHz. The every ε_r-T curves have two dielectric anomaly peaks. The low peak occurs at 80 °C, and the high peak is observed at 300 °C, which corresponds to the cubic-tetragonal phase transition temperature (T_c). The peak at the lower temperature is attributed to a FE-AFE phase transition in the BNT-BLZT system, while the peak at higher temperature is an AFE to paraelectric phase transition. It can be also observed that ε_r decreased with the increase of Zr content, meanwhile, they are also reflected in the corresponding loss tangent curves. These broad and frequency dependent peaks in dielectric permittivity and loss tangent indicate that BNT-BLZT samples exhibit obvious relaxor characteristics. The addition of Zr can improve the piezoelectric properties of BT-BNT ceramics.

4. Conclusions

Energy-storage properties of $[(Bi_{1/2}Na_{1/2})_{0.94}Ba_{0.06}]La_{(1-x)}Zr_x TiO_3$ (BNT-BLZT, $x=0$, 0.02, 0.04, 0.06) lead-free anti-ferroelectric ceramics fabricated via the conventional sintering technique were first investigated. XRD results show all ceramics possess a single perovskite structure phase, indicating that Zr^{4+} has diffused into the BNT-BLT lattices to form a solid solution. The P–E hysteresis loops of BNT-BLZT ceramics under different electric fields at 1 Hz can be observed that the saturation polarization P_s and the remnant polarization P_r are both decreased as Zr doped increasing, the P–E hysteresis loops of BNT-BLZT ceramics increasingly becomes more slant and slim, and the maximum electric field intensity E_{max} and the energy-storage density W is first increased and then decreased with the Zr doped increasing from 0 to 0.06, when $x=0.02$, the largest energy-storage density W_{max} is 1.58 J/cm^3, $E_c=83.4$ kV/cm. These properties indicate that BNT-BLZT ceramics are a promising lead-free anti-ferroelectric material for energy-storage capacitor application.

Acknowledgments

This work was supported by the grants from the Doctoral Program of Higher Education of China (20120131120032) and the National Natural Science Foundation of China (No. 51102181).

References

[1] AnKun Yang, ChangAn Wang, Rui Guo, Yong Huang, CeWen Nan, Effects of sintering behavior on microstructure and piezoelectric properties of porous PZT ceramics, Ceramics International 36 (2010) 549–554.
[2] B.J. Chu, X. Zhou, K.L. Ren, B. Neese, M.R. Lin, Q. Wang, F. Bauer, Q. M. Zhang, A dielectric polymer with high electric energy density and fast discharge speed, Science 313 (2006) 334.
[3] G.R. Love, Energy-storage in ceramic dielectrics, Journal of the American Ceramic Society 73 (1990) 323–334.
[4] H. Ogihara, C.A. Randall, S. Trolier-Mckinstry, High-energy density capacitors utilizing $0.7BaTiO_3$–$0.3BiScO_3$ ceramics, Journal of the American Ceramic Society 92 (2009) 1719–1743.
[5] Q.M. Zhang, L. Wang, J. Luo, Q. Tang, J. Du, Improved energy storage density in barium strontium titanate by addition of BaO–SiO_2–B_2O_3 glass, Journal of the American Ceramic Society 92 (2009) 1871–1874.
[6] X.F. Chen, X.L. Dong, G.S. Wang, F. Cao, Y.L. Wang, Doped Pb(Zr, Sn, Ti)O_3 slim-loop ferroelectric ceramics for high-power pulse capacitors application, Ferroelectrics 363 (2008) 56–63.
[7] I. Burn, D. Smyth, Energy storage in ceramic dielectrics, Journal of Materials Science 7 (1972) 339–348.
[8] Q. Xiao Bao, L. Hui Zhu, Q. Wei Huang, J. XV, Preparation of texture $Ba_2NaNb_5O_{15}$ ceramics by templated grain growth, Ceramics International 32 (2006) 745–749.
[9] S.T. Zhang, A.B. Kounga, W. Jo, C. Jamin, K. Seifert, T. Granzow, J. Rodel, D. Damjanovic, High-strain lead-free antiferroelectric electrostrictors, Advanced Materials 21 (2009) 4716–4736.
[10] R. Dittmer, W. Jo, D. Damjanovic, J. Rodel, Lead-free high-temperature dielectrics with wide operational range, Journal of Applied Physics 109 (3) (2011) 034107.
[11] X.R. Cheng, M.R. Shen, Enhanced spontaneous polarization in Sr and Ca co-doped $BaTiO_3$ ceramics, Solid State Communications 141 (2007) 587–599.
[12] K. Yang, C.L. Wang, J.C. Li, C. Zhang, R.Z. Zhang, Y.F. Zhang, Q. Z. Wu, Y.G. Lv, N. Yin, Structural and polarization properties of short-period $SrZrO_3/SrTiO_3$ superlattices, Physical Review 75 (22) (2007) 224117.
[13] H.L. Zhang, X.F. Chen, F. Cao, G.S. Wang, X.L. Dong, Z.Y. Hu, T. Du, Charge–discharge properties of an antiferroelectric ceramics capacitor under different electric fields, Journal of the American Ceramic Society 93 (12) (2010) 4015–4027.
[14] J. Kling, X.L. Tan, W. Jo, H.J. Kleebe, H. Fuess, J. Rodel, In-situ transmission electron microscopy of electric field-triggered reversible domain formation in Bi-based lead-free piezoceramics, Journal of the American Ceramic Society 93 (9) (2010) 2452–2459.
[15] M. Hinterstein, M. Knapp, M. Holzel, W. Jo, A. Cervellino, H. Ehrenberg, H. Fuessa, Field-induced phase transition in $Bi_{1/2}Na_{1/2}TiO_3$–based lead-free piezoelectric ceramics, Journal of Applied Crystallography 43 (2010) 1314–1335.
[16] Y. Hiruma, K. Yoshi, H. Nagata, T. Takenaka, Investigation of phase transition temperatures on $(Bi_{1/2}Na_{1/2})TiO_3$-$(Bi_{1/2}K_{1/2})TiO_3$ and $(Bi_{1/2}Na_{1/2})TiO_3$–$BaTiO_3$ Lead-free piezoelectric ceramics by electrical measurements, Ferroelectrics 346 (2007) 114–123.
[17] Q. Xiao Bao, L. Hui Zhu, Q. Wei Huang, J. XV, Preparation of texture $Ba_2NaNb_5O_{15}$ ceramics by templated grain growth, Ceramics International 32 (2006) 745–749.
[18] A. Sanson, R.W. Whatmore, Properties of $Bi_4Ti_3O_{12}$–$(Na_{1/2}Bi_{1/2})TiO_3$ piezoelectric ceramics, Japanese Journal of Applied Physics 41 (11) (2002) 7127.
[19] Jiwei Zhai, Cheng Gao, Xi Yao, Zhengkui Xu, Haydn Chen, Enhanced dielectric tunability properties of $Ba(Zr_xTi_{1-x})O_3$ thin films using seed layers on $Pt/Ti/SiO_2/Si$ substrates, Ceramics International 34 (2008) 905–910.
[20] H. Idink, V. Srikanth, W.B. White, Raman study of low temperature phase transitions in bismuth titanate, $Bi_4Ti_3O_{12}$, Journal of Applied Physics 76 (1994) 1819.